

Hydroxamic Acid Derivatives of β -Carboline/Hydroxycinnamic Acid Hybrids Inducing Apoptosis and Autophagy through the PI3K/Akt/mTOR Pathways

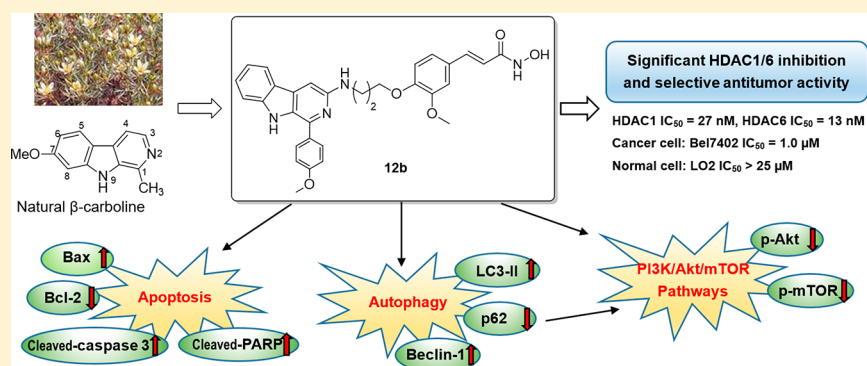
Yong Ling,^{*,†,‡,§} Yangyang Li,^{†,‡} Rui Zhu,[†] Jianqiang Qian,[†] Ji Liu,^{†,‡} Weijie Gao,[†] Chi Meng,[†] Jiefei Miao,^{†,‡} Biao Xiong,[†] Xiaodong Qiu,[†] Changchun Ling,^{†,‡} Hong Dai,^{*,§} and Yanan Zhang^{*,†}

[†]School of Pharmacy and Jiangsu Province Key Laboratory for Inflammation and Molecular Drug Target, Nantong University, Nantong 226001, People's Republic of China

[‡]The Affiliated Hospital of Nantong University, Nantong University, Nantong 226001, People's Republic of China

[§]College of Chemistry and Chemical Engineering, Nantong University, Nantong 226019, People's Republic of China

S Supporting Information



ABSTRACT: Naturally occurring β -carboline derivatives are known to have antitumor activities but with limited effectiveness. In order to improve their efficacy, a series of new hydroxamic-acid-containing β -carboline derivatives connected via a hydroxycinnamic acid moiety (12a–f) were developed to incorporate histone deacetylase (HDAC) inhibition for possible synergistic effects. When evaluated in *in vitro* assays, most of the analogues showed significant antitumor activities against four human cancer cells. In particular, 12b showed the highest cytotoxic potency of the series, including drug-resistant Bel7402 cells, but had minimal effect on normal hepatic LO2 cells. These compounds also showed excellent inhibitory effects against HDAC1/6, which appear to contribute greatly to their antiproliferative properties. Compound 12b enhanced the acetylation levels of histone H3 and α -tubulin and induced greater cancer cell apoptosis than the FDA-approved HDAC inhibitor SAHA by regulating expression of apoptotic proteins Bax, Bcl-2, and caspase 3. Importantly, 12b also induced a significant amount of autophagic flux activity in Bel7402 cells by increasing the expression of Beclin-1 and LC3-II proteins and decreasing that of LC3-I and p62. Finally, 12b significantly inhibited PI3K/Akt/mTOR signaling, an important cell-growth-promoting pathway aberrantly activated in many cancers. Together, the results suggest that these hydroxamic-acid-containing β -carboline derivatives may be new leads for the discovery of agents for the treatment of human carcinoma cancers.

Natural products have historically been a main source of drugs for the treatment of various diseases including cancers. Approximately 25% of all current drugs are derived from plants, and many others are synthetic analogues built upon prototype compounds isolated from plants.^{1,2} Many medicinal plant-based medicines, such as the camptothecin derivatives and taxanes (e.g., Taxol), are still an essential part of the armament for treating cancers, and natural products continue to provide leads for drug candidates that have entered clinical trials as anticancer agents.^{3,4}

Despite these advances, malignant tumors remain a serious threat to human health.⁵ According to the WHO, cancer is the second most frequent cause of death among the non-

communicable diseases, after cardiovascular disease. The number of cancer deaths accounts for about 13% of the world's total deaths, and more than 8.2 million people died of cancer in 2014.⁶ Chemotherapy remains the principal treatment for most human cancers; however, many of the current chemotherapeutic agents suffer from limitations including systemic toxicity, low selectivity, and drug resistance,^{7–9} making the discovery of new chemodrugs an urgent need.

Received: October 11, 2018

Naturally occurring β -carbolines, including harmine, harmaline, harmalol, and harmane, are indole alkaloids with a planar tricyclic 9H-pyrido[3,4-b]indole skeleton (Figure 1). Originally

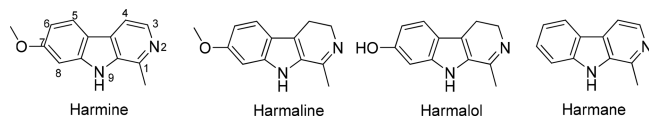


Figure 1. Structures of natural β -carbolines harmine, harmaline, harmalol, and harmane.

isolated from the plant *Peganum harmala* (Syrian rue, family Zygophyllaceae), β -carbolines are also known as harmala alkaloids, occurring in *Peganum harmala* in concentrations of 2–7% or even higher.¹⁰ The crude extract of *Peganum harmala* has been traditionally used as an herbal medicine in Central Asia, the Middle East, and North Africa because of its antibacterial effect and also in clinical treatment of cancer due to its inhibitory effects of cancer cells.^{11,12} Indeed, β -carbolines have been indicated in a range of diverse biological processes, including antitumor, antiviral, antimicrobial, and antiparasitic activities.^{13–15} β -Carbolines have attracted attention for the treatment of cancer due to their intercalation into DNA, inhibition of CDK and topoisomerase, and antiangiogenesis activity.^{16–18} In particular, β -carbolines such as harmine, were found to reduce resistance to several common anticancer drugs such as mitoxantrone and camptothecin.¹⁸ However, these β -carbolines show only modest efficacy as anticancer drugs and have often been used in combination with other anticancer agents to improve effectiveness.^{19,20}

Multitarget drugs comprising hybrids that combine structural components of two or more active drugs have been a promising strategy to generate potential leads that target multiple signaling pathways, therefore leading to improved biological activities and therapeutic efficacies.^{21,22} This approach is consistent with the traditional use of medicinal plants in cancer treatment, which, unlike pharmacological drugs, commonly contain a mixture of components that may act simultaneously on multiple protein targets. To this end, we envisioned the introduction of a hydroxamic acid functionality to the β -carboline, the former being an active fragment in many histone deacetylase (HDAC) inhibitors including suberanilohydroxamic acid (vorinostat, SAHA), an FDA approved drug (Figure 2). HDACs are a class of promising therapeutic targets for cancer intervention due to their involvement in gene transcription, cell cycle progression, and cell apoptosis and their overexpression in a variety of human tumors.²³ A variety of HDAC inhibitors have been approved

for the treatment of multiple cancers, particularly cutaneous T cell lymphoma (CTCL),²⁴ but are generally less effective toward solid tumors. Given the antitumor effects of β -carbolines on DNA damage and drug resistance, incorporation of an HDAC inhibitory hydroxamic acid fragment into the natural β -carbolines may lead to hybrid molecules with increased anticancer potency/efficacy or even reversal of drug resistance to a broader range of cancer, even solid tumors.

Finally, the hydroxamic acid functionality from HDAC inhibitors could readily be connected to β -carbolines using a hydroxycinnamic acid (HCA) structural moiety. HCAs including ferulic acid (FA) and 4-hydroxycinnamic acid (Figure 2), widely occur in plants and show antiproliferative activity against several types of cancer cells.^{25–27} HCAs and their derivatives have also been shown to block the transcription factor (NF- κ B) pathway and trigger an apoptotic cascade.^{28,29} In addition, *N*-hydroxycinnamamide, the hydroxamic acid analogue of HCA, is present in several FDA-approved HDAC inhibitors such as belinostat (PXD101) and panobinostat (LBH589) (Figure 2),^{30,31} thus making HCA an ideal connector for the hybrids. In addition to linking β -carbolines and the hydroxamic acid functionality, the HCA moiety may potentially contribute to the anticancer effects of the hybrids.

Herein, the synthesis and biological evaluation of the new β -carboline/HCA hybrids (12a–f, Figure 3), including the

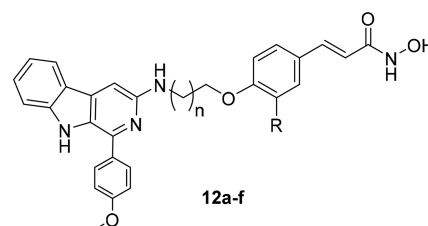


Figure 3. Hybrids based on β -carboline/HCA with hydroxamic acid functionality.

investigation of their potency and antitumor mechanisms such as tumor cell apoptosis induction and autophagy in several cancer cell lines, are reported. In view of the above discussion, we hypothesized that these hybrids, formed via conjugating the natural β -carboline with a hydroxamic acid using HCA as a linker, could display synergistic effects and improve anticancer activities.

RESULTS AND DISCUSSION

The tricyclic ring system of β -carboline alkaloids is commonly constructed by a Pictet–Spengler reaction between trypto-

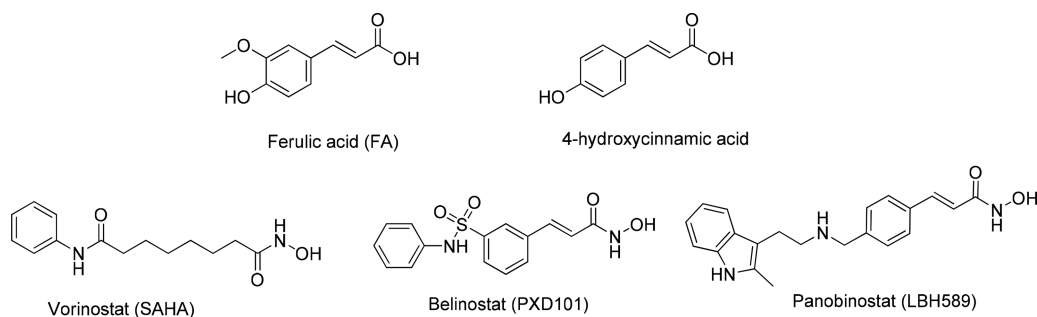
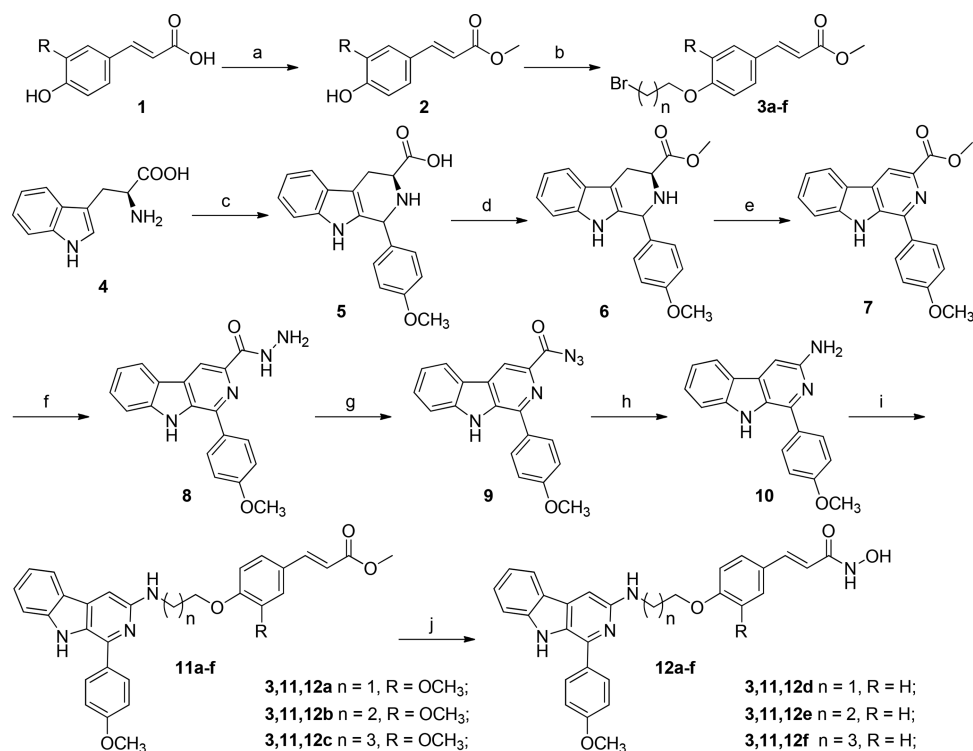


Figure 2. Hydroxycinnamic acids (HCA) and representative hydroxamic-acid-containing HDAC inhibitors.

Scheme 1^a

^aReagents and conditions: (a) thionyl chloride, MeOH, 0 °C, 1 h, and then 65 °C, 4 h; (b) ω -dibromoalkane, K_2CO_3 , CH_3CN , reflux, 4 h; (c) 4-methoxybenzaldehyde, HOAc, reflux, 4 h; (d) thionyl chloride, MeOH, 0 °C, 1 h, and then 65 °C, 6 h; (e) $KMnO_4$, DMF, rt, 5 h; (f) hydrazine monohydrate, MeOH, 50 °C, 6 h; (g) $NaNO_2$, HCl; (h) HOAc, H_2O , 50 °C, 6 h; (i) K_2CO_3 , CH_3CN , reflux, 12 h; (j) NH_2OK , MeOH, rt, 8–12 h.

Table 1. IC_{50} Values of 12a–f against Four Human HCC Cells and HDAC1

compd	in vitro antiproliferative activity (IC_{50}^a , μM)				HDAC1 (IC_{50} , nM)
	SMMC-7721	HepG2	Bel7402	Huh7	
SAHA	5.2 ± 0.5	5.9 ± 0.7	4.7 ± 0.6	5.1 ± 0.6	142 ± 18
harmine	47.6 ± 5.1	53.6 ± 5.5	ND ^b	ND	>1000
12a	4.0 ± 0.5	4.8 ± 0.6	1.8 ± 0.2	2.8 ± 0.3	32 ± 3
12b	2.9 ± 0.3	1.4 ± 0.3	1.0 ± 0.1	1.1 ± 0.2	27 ± 3
12c	7.1 ± 0.6	5.3 ± 0.6	4.6 ± 0.5	6.2 ± 0.2	61 ± 7
12d	6.3 ± 0.7	5.8 ± 0.6	5.2 ± 0.6	ND	75 ± 8
12e	4.1 ± 0.4	3.4 ± 0.4	4.0 ± 0.5	ND	57 ± 7
12f	>12.5	9.5 ± 1.1	8.9 ± 1.0	ND	125 ± 13

^aRelated data appeared as the means ± SD of three separate assays. ^bND: not detected.

phan and aldehydes. This strategy was used to prepare target compounds 12a–f as outlined in Scheme 1. First, the cinnamates 3a–f were prepared by esterification of hydroxycinnamic acid 1a or 1b with $SOCl_2$ in CH_3OH to afford methyl esters 2a,b. Treatment with ω -dibromoalkanes in the presence of K_2CO_3 afforded the appropriate ethers 3a–f. On the other hand, L-tryptophan (4) was converted to tetrahydrocarboline 5 in a Pictet–Spengler reaction with 4-methoxybenzaldehyde. Compound 5 was esterified by treatment with $SOCl_2$ in CH_3OH to give methyl ester 6, which was subsequently oxidized with $KMnO_4$ in dimethylformamide (DMF) to afford compound 7. Compound 7 was reacted with hydrazine hydrate to afford hydrazide 8. Hydrazide 8 was transformed to acyl azide 9 using $NaNO_2$. Curtius rearrangement of acyl azide 9 was carried out in aqueous HOAc to give compound 10. Reaction between 10 and bromides 3a–f in the

presence of K_2CO_3 in CH_3CN afforded the key intermediates 11a–f. Finally, treatment of 11a–f with NH_2OK afforded the target compounds 12a–f. These compounds were purified by silica gel column chromatography, and their structures were validated by MS, 1H NMR, ^{13}C NMR, and HRMS data. The compounds had a purity of >95% as determined by HPLC.

In order to obtain their cancer cell growth inhibitory activity, the target compounds 12a–f were first tested against four human hepatocellular carcinoma (HCC) cells (Bel7402, SMMC-7721, Huh7, and HepG2) in MTT assays. These cells were chosen to investigate how these hybrids would inhibit the growth of solid tumors, against which HDAC inhibitors are generally not effective. Since harmine has been shown to reduce resistance to some anticancer drugs, drug-sensitive Bel7402 cells, which are innately resistant to chemodrugs including doxorubicin and vincristine,³² were

also included. Harmine and the FDA-approved HDAC inhibitor for CTCL, SAHA, were tested in parallel. As shown in Table 1, compounds **12a–f** were all good antiproliferative agents, displaying IC_{50} values in the low micromolar range in all four human cancer cell lines. These IC_{50} values are significantly lower than that of harmine, and most of them were similar to or even lower than SAHA. Particularly, **12b** had IC_{50} values of 1.0 and 1.1 μ M in Bel7402 and Huh7 cells, respectively, which were 5-fold lower than those of SAHA ($IC_{50} = 4.7$ and 5.1 μ M).

It appears that compounds **12a–c** based on ferulic acid (R = OMe) were more potent in antiproliferation than the corresponding 4-hydroxycinnamic-acid-based **12d–f** (R = H). As for the methylene groups connecting the β -carboline and HCA, compounds with propyl ($n = 3$) groups exhibited greater antitumor activities than for ethyl ($n = 2$) and butyl ($n = 4$) analogues.

Compound **12b** was the most active compound of the series and was further evaluated for its selectivity profile against normal cells by determining its growth inhibitory effects on drug-sensitive HCC Bel7402 cells, drug-resistant HCC Bel7402/5-FU cells, and normal liver LO2 cells. Treatment with an increasing dose of **12b** displayed little effect on the survival of nontumor LO2 cells; however, the same treatment induced substantial inhibition of both Bel7402 and Bel7402/5-FU cell proliferation (Figure 4). These findings suggest that **12b** is selective in the antiproliferation of tumor cells over normal cells.

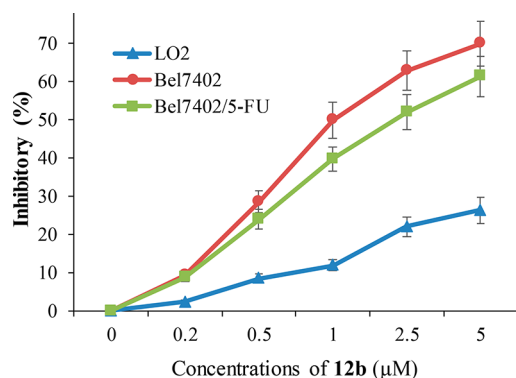


Figure 4. Inhibitory effects of **12b** on the proliferation of Bel7402, Bel7402/5-FU, and LO2 cells. Cells were incubated with different concentrations of **12b** for 72 h. Cell inhibitory % was determined using the MTT assay. These data are from three independent experiments and are presented as the mean \pm SD.

All targets were tested for their inhibitory effects on HDAC1 protein in the enzymatic fluorimetric activity assay. HDAC1 is a member of the HDAC family important for cell proliferation and tissue development and is routinely targeted for cancer treatment. While harmine showed little activity at HDAC1 ($IC_{50} > 1000$ nM), compounds **12a–f** all showed potencies similar to or greater than SAHA (Table 1). This confirms that the presence of the hydroxamic acid induced HDAC activities. Interestingly, the relative HDAC1 potencies matched well with their cell-based antiproliferation results. The lower potencies of these compounds in cell antiproliferation, which were in the μ M range, compared to nM potencies in HDAC inhibition, are likely the result of their interactions with other proteins present in the cells, rendering lowered effective concentrations for HDACs. These results suggest that the HDAC inhibitory

activities contribute greatly to the antiproliferative properties of this series of hybrids.

Since other members of the HDAC family have been indicated in cancers, compounds **12a** and **12b**, two of the most potent compounds of the series inhibiting HDAC1, were tested for their potencies against HDAC3, -6, and -8 by determining the fluorescent-based activity using recombinant human enzymes. SAHA was again tested in parallel. As summarized in Table 2, **12a** and **12b** both showed good

Table 2. IC_{50} Values of Compounds **12a,b** against HDAC1, HDAC3, HDAC6, and HDAC8

compound	IC_{50} (nM) ^a			
	HDAC1	HDAC3	HDAC6	HDAC8
SAHA	142 \pm 18	153 \pm 17	65 \pm 7	425 \pm 51
12a	32 \pm 3	125 \pm 15	17 \pm 3	>1000
12b	27 \pm 3	148 \pm 16	13 \pm 2	>1000

^aThese data are from three independent experiments and are expressed as the mean \pm SD.

inhibitory potencies against HDAC6 with IC_{50} values of 16 and 13 nM, respectively. These values are about 2-fold lower than HDAC1, and 7- to 11-fold lower than HDAC3. Neither **12a** nor **12b** showed much activity against HDAC8 ($IC_{50} > 1000$ nM). Importantly, the IC_{50} values of **12b** were about 5-fold lower than those of SAHA on both HDAC1 and HDAC6.

HDACs deacetylate histones and suppress gene expression, and therefore inhibition of HDACs at the cellular level would increase acetylation of histones. Expression levels of acetylated histone H3 and α -tubulin, biomarkers of HDAC inhibition, were determined upon treatment with **12b** in Western blot assays (Figure 5). Bel7402 cells were thus incubated with either the vehicle, SAHA (5.0 μ M), or **12b** (1.0 and 3.0 μ M) for 72 h. Compound **12b** significantly enhanced histone H3

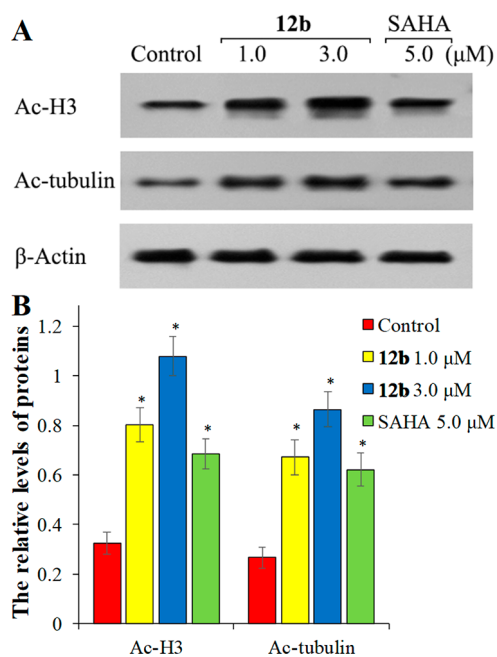


Figure 5. Immunoblot analysis of Ac-histone H3 and Ac- α -tubulin in vitro. (A) Western blot analysis of Bel7402 cells treated with **12b** and SAHA. (B) Quantitative analysis. Related data appear as means \pm SD of three separate assays. * $P < 0.01$ vs control.

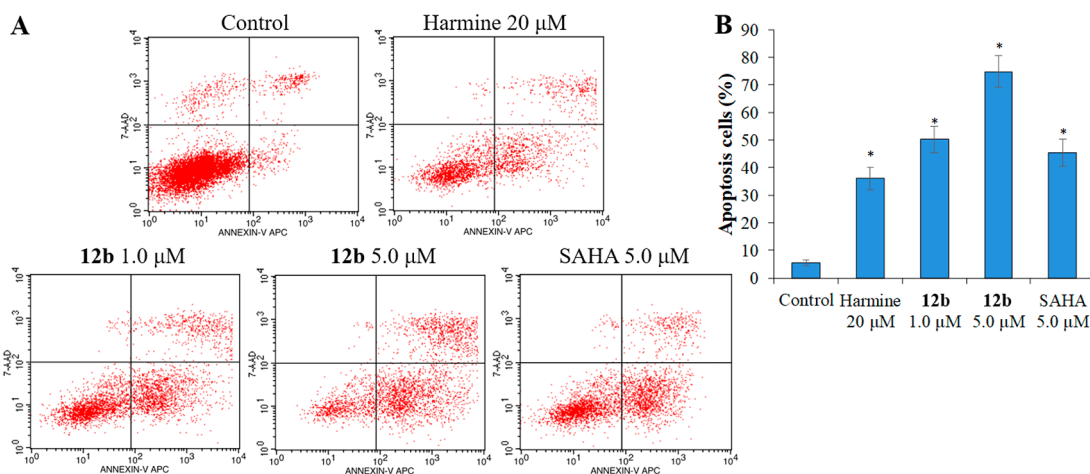


Figure 6. Compound **12b** induces Bel7402 cell apoptosis in vitro. (A) Flow cytometry analysis of Bel7402 cells treated with **12b**, SAHA, or harmine, respectively, and stained with FITC-annexin V/PI. (B) Quantitative analysis of percentages of apoptotic cells. Related data appear as means \pm SD of three separate assays. * $P < 0.01$ vs control.

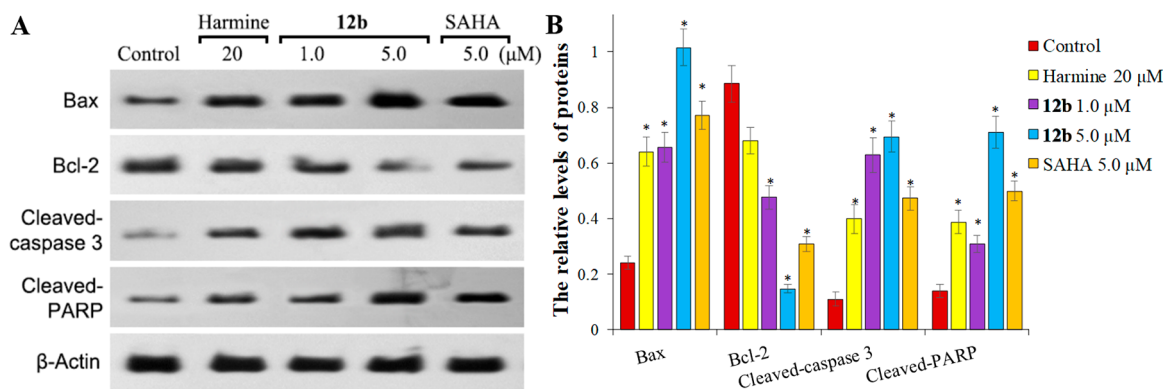


Figure 7. (A) Expression levels of Bcl-2, Bax, cleaved-caspase 3, cleaved-PARP, and β -actin as determined by Western blot analysis using Bel7402 cells treated with vehicle, **12b**, harmine, or SAHA. (B) Relative levels of each protein (Bcl-2, Bax, cleaved-caspase 3, and cleaved-PARP) compared to β -actin. Related data appear as the means \pm SD of three separate assays. * $P < 0.01$ vs control.

acetylation and also increased the Ac- α -tubulin expression level in a dose-dependent fashion, suggesting HDAC inhibitor. The Ac-histone H3 and Ac- α -tubulin levels in the **12b**-treated groups were similar (1.0 μ M) or even higher (3.0 μ M) than the 5.0 μ M SAHA-treated group, agreeing with their HDAC isoform enzymatic activities.

Apoptosis is a process critically involved in tumor formation and treatment responses.^{33–35} Since it showed significant HCC cell antiproliferative activities and also selectively inhibited HDAC1/6, **12b** was assessed for its ability to enhance cancer cell apoptosis. Thus, Bel7402 cells were treated with either SAHA, harmine, or **12b** for 72 h, and the apoptotic rates of cells were analyzed using FITC-annexin V/PI staining and flow cytometry. As shown in Figure 6, cells exposed to increasing concentrations of **12b** displayed higher percentages of annexin V + apoptotic Bel7402 cells (49.6% for 1.0 μ M and 73.8% for 5.0 μ M). These results were higher than the SAHA (45.4% for 5.0 μ M) and harmine (36.1% for 20 μ M) groups at the same or higher concentrations. Therefore, **12b** induced Bel7402 cell apoptosis with greater potency than both SAHA and harmine.

Caspase-3 is a member of the cysteine–aspartic acid protease (caspase) family and is closely associated with apoptosis. In most cells caspase 3 is normally expressed in an inactive pro-enzyme form, but upon activation, it can often activate other procaspases, triggering a protease cascade.³⁶ To

evaluate **12b** for its apoptosis induction effect, the expression levels of apoptotic proteins Bax and Bcl-2 and the cleavage states of caspase-3 and poly ADP ribose polymerase (PARP, an apoptosis marker)³⁷ upon treatment with **12b** (Figure 7) were evaluated. Subconfluent Bel7402 HCC cells were treated with vehicle or **12b** for 72 h, and the cells were lysed and subjected to analysis by Western blot. As shown in Figure 7A, treatment with **12b** markedly increased the proapoptotic Bax levels but decreased the antiapoptotic Bcl-2 levels in a dose-dependent fashion. Additionally, compound **12b** led to cleavage of both caspase-3 and PARP, both more significant than the control group and the SAHA-treated group. Accordingly, these immunohistochemical analyses confirmed that treatment with **12b** induced tumor cell apoptosis by regulating apoptotic-related protein levels in Bel7402 cells.

Autophagy, the natural, regulated process that the cell uses to disassemble unnecessary or dysfunctional components, is considered a promising and novel strategy to enhance antitumor efficacy of chemotherapy drugs.^{38,39} To investigate whether **12b** induced autophagy in Bel7402 cells, acridine orange (AO) staining was used to detect autophagic formation using fluorescence microscopy. As shown in Figure 8, in control cells green fluorescence was primarily emitted with only weak red fluorescence, indicating a low autophagic induction. On the other hand, Bel7402 cells treated with **12b**

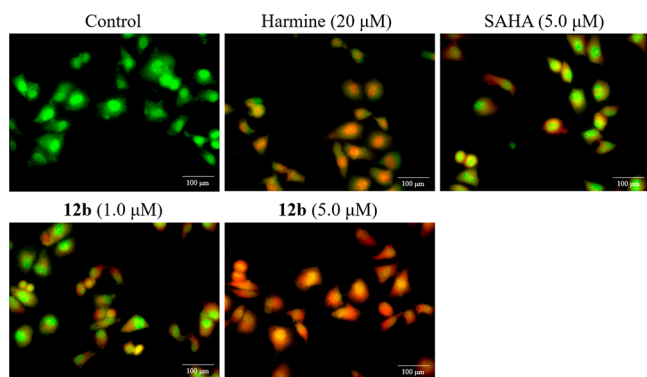


Figure 8. Detection of autophagic vacuoles in Bel7402 cells after various treatments for 24 h: (a) control cells; (b) harmine at 20 μM ; (c) SAHA at 5.0 μM ; (d) 1.0 μM **12b**-treated cells; and (e) 5.0 μM **12b**-treated cells. The level of acridine orange staining was determined by fluorescence microscopy. Representative images were captured from three independent experiments under 400 \times magnification.

displayed an increase in red fluorescence with the increase of drug concentration, while the green fluorescence intensity decreased. These results suggest a significant amount of autophagic flux activity in **12b**-treated groups in Bel7402 cells, more significant than the harmine- and SAHA-treated groups.

Next, the ability and mechanism of **12b** in induction of autophagy were further investigated by determining the levels of several important autophagy-associated proteins. The transformation of LC3-I into LC3-II is a key step in autophagy, and the number of LC3-II puncta correlates with the number of autophagosomes. Thus, the expression of LC3-I, LC3-II, p62, and Beclin-1, proteins all related to autophagy, in response to **12b** treatment was examined (Figure 9). Western blot assay showed a substantial increase in LC3-II and Beclin-1 protein expression levels, whereas the expression of p62 and LC3-I was reduced upon treatment with **12b** of different concentrations. The expression of LC3-II in **12b**-treated groups was higher than that of the SAHA-treated group (Figure 9B).

The PI3K/Akt/mTOR pathway is an essential signaling pathway in the regulation of the cell cycle, and its aberrant activation promotes tumor cell survival and proliferation in many cancers.⁴⁰ Once PI3K activates the serine/threonine kinase Akt, Akt will then phosphorylate and activate the serine/threonine kinase mTOR through a series of regu-

lators.⁴¹ To further study the underlying molecular mechanisms of **12b**, the effects of **12b** on regulating PI3K/Akt/mTOR signaling in Bel7402 cells, using SAHA and harmine as controls, were investigated. Thus, Bel7402 cells were treated with harmine, SAHA, or **12b** at 1.0 and 2.5 μM , and the expression and activation of Akt and mTOR were analyzed by Western blotting. Interestingly, treatment with **12b** significantly inhibited the phosphorylation of both Akt and mTOR in a dose-dependent manner, whereas it did not change the expression levels of these two proteins in these cancer cells (Figure 10). Similarly, treatment with SAHA and harmine also effectively reduced the levels of Akt and mTOR phosphorylation, although to a lesser extent compared to **12b**. These results suggest that treatment with **12b** could significantly inhibit PI3K/Akt/mTOR signaling, thus generating highlighted anticancer effects.

In summary, we report a new series of hydroxamic-acid-based β -carboline/hydroxycinnamic acid hybrids, **12a–f**, which incorporate the key structural components of harmine, classical HDACIs, and HCA. While HDAC inhibitors are generally not effective against solid tumors and β -carboline possesses weak anticancer activities, a combination of these components may lead to synergistic effects and thus improved efficacy or even drug resistance reversal. These hybrids were evaluated for their biological activities and anticancer mechanisms in a battery of in vitro assays. Most of the compounds displayed significant antiproliferative activity with IC_{50} values in the low micromolar range. In particular, **12b** selectively inhibited tumor cell proliferation of drug-sensitive Bel7402 and drug-resistant Bel7402/5-FU cells, but not normal LO2 cells. These hybrids appeared to retain HDAC inhibitory effects, and both **12a** and **12b** exerted selective HDAC1/6 inhibition. Treatment with **12b** resulted in enhancement of acetylated histones and acetylated α -tubulin protein levels and promoted cell apoptosis by enhancing the expression of cleaved caspase-3 and PARP in Bel7402 cells. In addition, **12b** also induced a significant amount of autophagic flux activity in Bel7402 cells by the upregulation of LC3-II and Beclin-1 proteins and downregulation of p62 and LC3-I. Finally, **12b** could significantly inhibit PI3K/Akt/mTOR signaling, thus generating highlighted anticancer effects. Given their antitumor activities, particularly against drug-sensitive and -resistant cancer cells, these β -carboline/hydroxamic acid hybrids may warrant further evaluation as potential candidates for the treatment of human cancer.

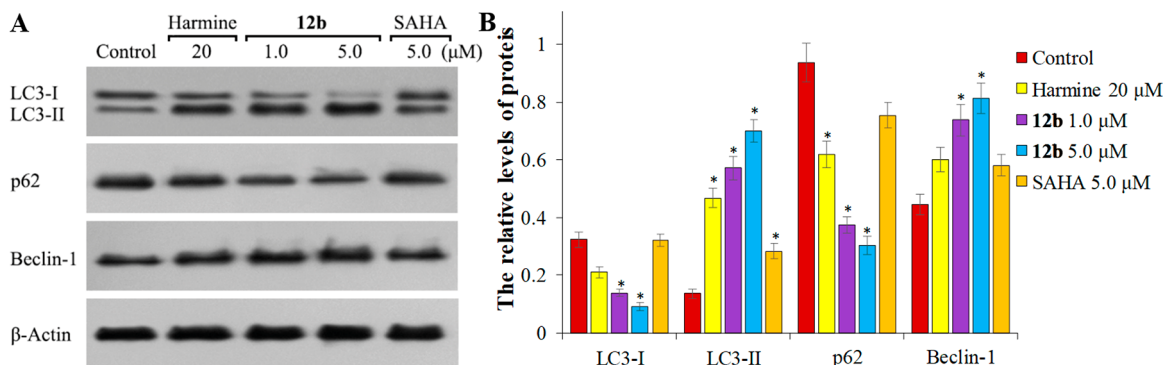


Figure 9. (A) Expression levels of autophagy-related proteins LC3, p62, and beclin-1 as determined by Western blot analysis in Bel7402 cells treated with vehicle, **12b**, harmine, or SAHA. (B) Quantitative analysis of LC3, p62, and beclin-1 levels relative to control β -actin. Related data appeared as the means \pm SD of three separate assays. * $P < 0.01$ vs respective control.

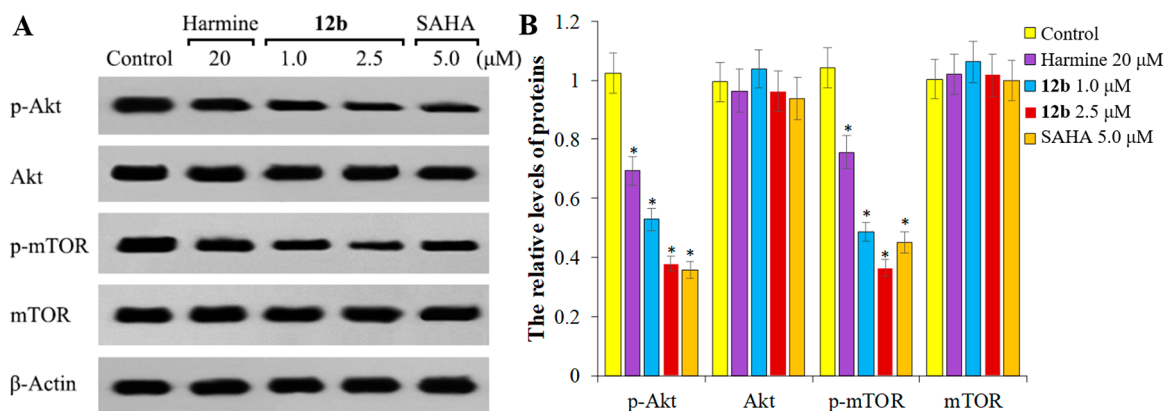


Figure 10. Effects of **12b** on the PI3K/Akt/mTOR signaling in Bel7402 cells. (A) Levels of Akt and mTOR expression and phosphorylation relative to β -actin by Western blot analysis. (B) Quantitative analysis. Related data appear as the means \pm SD of three separate assays. * $P < 0.01$ vs the vehicle-treated control.

EXPERIMENTAL SECTION

General Experimental Procedures. ^1H and ^{13}C NMR spectra were collected on a Bruker AV 400 M spectrometer in $\text{DMSO-}d_6$ or CDCl_3 , and tetramethylsilane was used as the internal standard. Mass spectra was recorded on a Mariner mass spectrometer (ESI). HRMS data were acquired with an Agilent Technologies LC/MSD TOF. HCA (**1**), *L*-tryptophan (**4**), and 4-methoxybenzaldehyde were purchased from Aladdin (Shanghai, China). Compounds **2** and **6–10** were prepared according to literature procedures.⁴²

Preparation of 3a–f. Compound 3a. To a solution of 1,2-dibromoethane (2.78 g, 15 mmol) were added compound **2a** (2.08 g, 10 mmol) and K_2CO_3 (2.75 g, 20 mmol). The mixture was stirred at 70 °C for 4 h. The mixture was concentrated, and the residue was collected through extraction and concentration and further purified through column chromatography (petroleum ether/EtOAc = 15:1) to afford a colorless oil. Yield: 73.1%. MS (ESI) $m/z = 315$ [$\text{M} + \text{H}$]⁺.

Compound 3b. Refer to **3a**; compound **3b** was synthesized starting from **2a** and 1,3-dibromopropane to give a light yellow oil. Yield: 68.0%. MS (ESI) $m/z = 329$ [$\text{M} + \text{H}$]⁺.

Compound 3c. Refer to **3a**; compound **3c** was synthesized starting from **2a** and 1,4-dibromobutane to give a light yellow oil. Yield: 70.1%. MS (ESI) $m/z = 343$ [$\text{M} + \text{H}$]⁺.

Compound 3d. Refer to **3a**; compound **3d** was synthesized starting from **2b** and 1,2-dibromoethane to give a light yellow oil. Yield: 75.2%. MS (ESI) $m/z = 285$ [$\text{M} + \text{H}$]⁺.

Compound 3e. Refer to **3a**; compound **3e** was synthesized starting from **2b** and 1,3-dibromopropane to give a light yellow oil. Yield: 69.4%. MS (ESI) $m/z = 299$ [$\text{M} + \text{H}$]⁺.

Compound 3f. Refer to **3a**; compound **3f** was synthesized starting from **2b** and 1,4-dibromobutane to give a light yellow oil. Yield: 66.1%. MS (ESI) $m/z = 313$ [$\text{M} + \text{H}$]⁺.

Preparation of 12a–f. Compound 12a. Compound **10** (2.89 g, 10 mmol), K_2CO_3 (2.75 g, 20 mmol), and **3a** (3.14 g, 10 mmol) were added to CH_3CN (40 mL), and the mixture was stirred at 55 °C for 12 h. The mixture was concentrated, and the residue was diluted with H_2O and extracted with EtOAc (2 \times 50 mL). The combined EtOAc solvent was dried over Na_2SO_4 , filtered, and concentrated. The residue was dissolved in a solution of NH_2OK (2.8 g, 40 mmol) in anhydrous MeOH (50 mL) and stirred for 8–12 h. Upon completion of the reaction, the mixture was concentrated, and the residue was collected through extraction and concentration and further purified through quick column chromatography to produce a light yellow solid. Yield: 52%. MS (ESI) $m/z = 525$ [$\text{M} + \text{H}$]⁺; ^1H NMR ($\text{DMSO-}d_6$, 400 MHz) δ 11.75 (s, 1H, NH), 8.63 (s, 1H, NH), 8.39 (d, 1H, $J = 8.0$ Hz, Ar-H), 7.96 (m, 4H, Ar-H), 7.52 (m, 7H, Ar-H, NH, CH), 6.96 (m, 2H, Ar-H), 6.53 (d, 1H, $J = 16.0$ Hz, Ar-H), 4.27 (m, 2H, CH_2), 3.88 (s, 6H, OCH_3), 3.76 (m, 2H, CH_2); ^{13}C NMR ($\text{DMSO-}d_6$, 100 MHz) δ 167.4, 151.3, 149.9, 149.0, 146.0, 143.1, 142.1, 139.8, 134.8, 133.7, 131.3, 130.3, 128.6, 128.0, 127.5, 127.2, 126.0, 123.0,

122.0, 121.3, 118.9, 117.5, 113.5, 112.5, 69.2, 57.0, 56.3, 42.9; HRMS (ESI) m/z calcd for $\text{C}_{30}\text{H}_{29}\text{N}_4\text{O}_5$ [$\text{M} + \text{H}$]⁺, 525.2138; found, 525.2153.

Compound 12b. Refer to **12a**; compound **12b** was synthesized starting from **10**, **3b**, and NH_2OK in a yield of 46%. MS (ESI) $m/z = 539$ [$\text{M} + \text{H}$]⁺; ^1H NMR ($\text{DMSO-}d_6$, 400 MHz) δ 10.62 (s, 1H, NH), 8.96 (s, 1H, NH), 8.02 (m, 4H, Ar-H), 7.45 (m, 4H, NH, Ar-H, CH), 7.13 (m, 6H, Ar-H), 6.34 (d, 1H, $J = 16.0$ Hz, =CH), 4.16 (m, 2H, CH_2), 3.85 (m, 6H, OCH_3), 3.50 (m, 2H, CH_2), 2.11 (m, 2H, CH_2); ^{13}C NMR ($\text{DMSO-}d_6$, 100 MHz) δ 167.1, 151.8, 149.7, 149.4, 145.2, 143.1, 141.6, 138.8, 134.6, 132.1, 130.5, 130.0, 129.5, 128.5, 127.7, 127.3, 126.0, 123.9, 121.6, 121.1, 119.0, 118.3, 114.2, 112.4, 68.0, 56.3, 55.8, 39.6, 30.4; HRMS (ESI) m/z calcd for $\text{C}_{31}\text{H}_{31}\text{N}_4\text{O}_5$ [$\text{M} + \text{H}$]⁺, 539.2294; found, 539.2307.

Compound 12c. Refer to **12a**; compound **12c** was obtained starting from **10**, **3c**, and NH_2OK in a yield of 49%; MS (ESI) $m/z = 553$ [$\text{M} + \text{H}$]⁺; ^1H NMR ($\text{DMSO-}d_6$, 400 MHz) δ 10.76 (s, 1H, NH), 8.00 (m, 3H, Ar-H), 7.43 (m, 5H, NH, Ar-H, CH), 7.09 (m, 6H, Ar-H, NH), 6.55 (d, 1H, $J = 16.0$ Hz, =CH), 5.98 (s, 1H, Ar-H), 4.07 (m, 2H, CH_2), 3.85 (m, 6H, OCH_3), 3.39 (m, 3H, OH, CH_2), 1.76–1.89 (m, 4H, 2 \times CH_2); ^{13}C NMR ($\text{DMSO-}d_6$, 100 MHz) δ 167.3, 151.8, 149.7, 149.4, 143.5, 141.9, 140.6, 138.8, 133.9, 133.1, 132.1, 130.5, 129.0, 128.5, 128.2, 127.8, 125.9, 123.3, 121.5, 121.1, 119.0, 117.7, 114.8, 112.3, 63.9, 56.3, 55.8, 38.7, 29.0, 23.0; HRMS (ESI) m/z calcd for $\text{C}_{32}\text{H}_{33}\text{N}_4\text{O}_5$ [$\text{M} + \text{H}$]⁺, 553.2451; found, 553.2442.

Compound 12d. Refer to **12a**; compound **12d** was obtained starting from **10**, **3d**, and NH_2OK in a yield of 55%. MS (ESI) $m/z = 495$ [$\text{M} + \text{H}$]⁺; ^1H NMR ($\text{DMSO-}d_6$, 400 MHz) δ 10.63 (s, 1H, NH), 8.01 (d, 1H, $J = 4$ Hz, Ar-H), 7.92 (m, 2H, Ar-H), 7.68 (m, 2H, Ar-H), 7.45 (m, 5H, NH, Ar-H, CH), 7.10 (m, 4H, Ar-H, NH), 6.60 (m, 3H, Ar-H, CH), 4.27 (m, 2H, CH_2), 3.85 (m, 4H, OCH_3 , OH), 3.76 (m, 2H, CH_2); ^{13}C NMR ($\text{DMSO-}d_6$, 100 MHz) δ 167.5, 152.8, 151.9, 145.5, 143.6, 143.3, 138.9, 134.1, 133.8, 133.3, 132.9, 132.0, 130.3, 130.0, 129.3, 128.6, 128.0, 121.5, 119.2, 114.8, 112.8, 69.1, 56.2, 43.9; HRMS (ESI) m/z calcd for $\text{C}_{29}\text{H}_{27}\text{N}_4\text{O}_4$ [$\text{M} + \text{H}$]⁺, 495.2032; found, 495.2023.

Compound 12e. Refer to **12a**; compound **12e** was obtained starting from **10**, **3e**, and NH_2OK in a yield of 56%. MS (ESI) $m/z = 509$ [$\text{M} + \text{H}$]⁺; ^1H NMR ($\text{DMSO-}d_6$, 400 MHz) δ 10.81 (s, 1H, NH), 8.07 (d, 1H, $J = 8.0$ Hz, Ar-H), 7.68 (m, 3H, Ar-H), 7.49 (m, 7H, NH, Ar-H, CH), 7.14 (m, 3H, Ar-H, NH), 6.68 (m, 3H, Ar-H, CH), 4.19 (m, 2H, CH_2), 3.85 (s, 3H, OCH_3), 3.50 (m, 2H, CH_2), 2.13 (m, 2H, CH_2); ^{13}C NMR ($\text{DMSO-}d_6$, 100 MHz) δ 165.7, 152.6, 151.9, 146.3, 143.4, 142.1, 139.9, 138.9, 134.1, 132.8, 132.4, 131.5, 130.4, 129.8, 129.2, 128.6, 127.9, 122.6, 121.8, 120.7, 113.9, 113.3, 67.7, 55.9, 38.2, 30.7; HRMS (ESI) m/z calcd for $\text{C}_{30}\text{H}_{29}\text{N}_4\text{O}_4$ [$\text{M} + \text{H}$]⁺, 509.2189; found, 509.2201.

Compound 12f. Refer to **12a**; compound **12f** was obtained starting from **10**, **3f**, and NH_2OK in a yield of 51%. MS (ESI) $m/z = 523$ [M

+ H]⁺; ¹H NMR (DMSO-*d*₆, 400 MHz) δ 10.76 (s, 1H, NH), 7.97–8.04 (m, 3H, Ar-H), 7.35–7.53 (m, 6H, NH, Ar-H, CH), 7.01–7.13 (m, 5H, Ar-H, NH), 6.77 (m, 1H, Ar-H), 6.57 (d, 1H, *J* = 16.0 Hz, = CH), 4.18 (m, 2H, CH₂), 3.86 (s, 3H, OCH₃), 3.50 (m, 2H, CH₂), 1.79–1.90 (m, 4H, 2 × CH₂); ¹³C NMR (DMSO-*d*₆, 100 MHz) δ 165.8, 152.6, 151.8, 145.3, 143.1, 142.1, 140.3, 138.2, 134.5, 132.6, 131.6, 130.2, 129.2, 128.8, 128.2, 128.0, 127.9, 122.6, 121.8, 120.8, 116.3, 113.2, 64.1, 56.1, 38.1, 28.6, 22.9; HRMS (ESI) *m/z* calcd for C₃₁H₃₁N₄O₄ [M + H]⁺, 523.2345; found, 523.2353.

Cell Culture. Human HCC cells Bel7402, HepG2, Huh7, and SMMC-7721 and liver normal cells LO2 were purchased from SICB (Shanghai Institute of Cell Biology, China). The cells were kept in Dulbecco's modified Eagle's medium (DMEM) (Gibco, NY, USA) possessing 10% heat-inactivated fetal bovine serum (FBS), streptomycin, and penicillin at 100 U/mL at 37 °C in a humid atmosphere with 5% CO₂ and 95% air. Cells were routinely subcultured twice weekly.

MTT Assay. Briefly, 100 μ L of appropriate cells (10⁴ cells/mL) was cultured in 96-well flat-bottom microplates in DMEM medium overnight. The cells were treated by adding 100 μ L of each compound into the respective well for 72 h. The negative control was a 0.1% DMSO aqueous solution. After 4 h of incubation, to each well was added 30 μ L of MTT (5 mg/mL), and the absorbance of each well was measured using an ELISA plate reader at 570 nm. The cytotoxicity potency of tested compounds was calculated according to the previous literature. All the IC₅₀ data were analyzed using GraphPadPrism software (version 4.03).

HDAC Assay. According to the directions of the HDAC1/3/6/8 fluorimetric assay kit (FLUOR DE LYS, USA), each compound at different concentrations was incubated with each HDAC enzyme in the presence of enzyme substrate (Boc-Lys (Ac)-AMC) at 37 °C for 60 min.⁴² The reaction was quenched by the addition of the lysine developer. After 30 min, the fluorimetric emission was measured in a fluorescence plate reader (excitation: 355 nm, emission: 460 nm). Each HDAC inhibitory rate was measured according to the percentage of activity relative to the control. All the IC₅₀ data were analyzed using GraphPadPrism software (version 4.03).

Cell Apoptosis Analysis by Flow Cytometry Assay. A total of 10 000 Bel7402 cells were cultured overnight and incubated with **12b** (1.0 and 5.0 μ M), SAHA (5.0 μ M), harmine (20 μ M), or vehicle for 72 h. The cells were harvested and stained with annexin-V APC and 7-AAD for 15 min. Flow cytometry analysis (Calibur, BD, USA) was used to measure the percentage of apoptotic cells, using the annexin-V APC signal (excitation: 633 nm, emission: 660 nm) and 7-AAD signal (excitation: 488 nm, emission: 647 nm). The data were analyzed through WinList 3D software (version 7.1), and the histogram was plotted using Excel (version 2016).

Acridine Orange Staining. A total of 10 000 cells were cultured overnight and incubated with **12b** (1.0, 5.0 μ M), SAHA (5.0 μ M), harmine (20 μ M), or vehicle for 72h. The cells were stained with 1 mg/mL AO for 15–20 min. The AO was then removed and visualized through a fluorescence microscope (ImageXpress Micro, MD, USA).

Western Blot Analysis. The activity of HDAC-related proteins, autophagy-related proteins, Akt, and mTOR was analyzed by the Western blot assay. Bel7402 cells (1.5 × 10⁵/mL) were treated with or without SAHA, **12b**, or harmine at indicated dosages for 24 or 72 h. The cell lysates (0.05 mg/lane) were separated by SDS-PAGE (12% gel) and transferred onto nitrocellulose membranes. When the reaction was blocked using 5% nonfat milk, the target proteins were then detected by different antibodies, such as anti-Bax, anti-Bcl-2, anti-acetyl-H3, anti-acetyl- α -tubulin, anti-LC3, anti-p62, anti-Akt, anti-phospho-Akt (Ser473), anti-mTOR, anti-phospho-mTOR, anti-beclin-1, and anti- β -actin antibodies (Cell Signaling Technology, MA, USA), respectively. The bound antibodies were detected by horse radish peroxidase-conjugated second antibodies and then visualized using the chemiluminescent reagent.

■ ASSOCIATED CONTENT

📄 Supporting Information

The Supporting Information is available free of charge on the ACS Publications website at DOI: 10.1021/acs.jnatprod.8b00843.

¹H NMR and ¹³C NMR spectra for **12a–f** (PDF)

■ AUTHOR INFORMATION

Corresponding Authors

*E-mail (Y. Ling): Lyyy111@sina.com.

*E-mail (H. Dai): dh123@ntu.edu.cn.

*Tel (Y. Zhang): +86-513-85051892. E-mail: zhangyanan@gmail.com.

ORCID

Yong Ling: 0000-0002-3373-011X

Notes

The authors declare no competing financial interest.

■ ACKNOWLEDGMENTS

This work was financially supported by the Project of “Jiangsu Six Peaks of Talent” (2016-SWYY-CXTD-008 and 2014-SWYY-044), China and Jiangsu Province Postdoctoral Science Foundation (2018T110533, 2016M590488, and 1601136B), the Project of “Jiangsu 333 High-Level Talents”, Applied Research Projects of Nantong City (MS12018079 and JC2018125), and the testing service was provided by Analysis and Testing Center in Nantong University.

■ REFERENCES

- Hostettmann, K. *Pure Appl. Chem.* **1999**, *70*.
- Chen, G. T.; Lu, Y.; Yang, M.; Li, J. L.; Fan, B. Y. *Phytother. Res.* **2018**, *32*, 823–864.
- Harvey, A. L.; Young, L. C.; Viljoen, A. M.; Gericke, N. P. *J. Ethnopharmacol.* **2011**, *137*, 1124–1129.
- McChesney, J. D.; Venkataraman, S. K.; Henri, J. T. *Phytochemistry* **2007**, *68*, 2015–22.
- Chen, J. G.; Kensler, T. W. *Chem. Res. Toxicol.* **2014**, *27*, 3–6.
- McGuire, S. *Adv. Nutr.* **2016**, *7*, 418–419.
- Longley, D. B.; Johnston, P. G. *J. Pathol.* **2005**, *205*, 275–92.
- Huang, J.; Mei, H.; Tang, Z.; Li, J.; Zhang, X.; Lu, Y.; Huang, F.; Jin, Q.; Wang, Z. *J. Controlled Release* **2017**, *245*, 1–14.
- Han, M. L.; Zhao, Y. F.; Tan, C. H.; Xiong, Y. J.; Wang, W. J.; Wu, F.; Fei, Y.; Wang, L.; Liang, Z. Q. *Acta Pharmacol. Sin.* **2016**, *37*, 1606–1622.
- Herraiz, T.; González, D.; Ancin-Azpilicueta, C.; Arán, V. J.; Guillén, H. *Food Chem. Toxicol.* **2010**, *48*, 839–43.
- Moloudizargari, M.; Mikaili, P.; Aghajanshakeri, S.; Asghari, M. H.; Shayegh, J. *Pharmacogn. Rev.* **2013**, *7*, 199–212.
- Lamchouri, F. *Plant Sci. Today* **2014**, *1*, 192–195.
- Han, X.; Zhang, J.; Guo, L.; Cao, R.; Li, Y.; Li, N.; Li, N.; Ma, Q.; Wu, J.; Wang, Y.; Si, S. *PLoS One* **2012**, *7*, No. e46546.
- Herraiz, T.; Gonzalez, D.; Ancin-Azpilicueta, C.; Aran, V. J.; Guillen, H. *Food Chem. Toxicol.* **2010**, *48*, 839–845.
- Chen, Q.; Chao, R.; Chen, H.; Hou, X.; Yan, H.; Zhou, S.; Peng, W.; Xu, A. *Int. J. Cancer* **2005**, *114*, 675–82.
- Hamsa, T. P.; Kuttan, G. *Eur. J. Pharmacol.* **2010**, *649*, 64–73.
- Carvalho, A.; Chu, J.; Meinguet, C.; Kiss, R.; Vandebussche, G.; Masereel, B.; Wouters, J.; Kornienko, A.; Pelletier, J.; Mathieu, V. *Eur. J. Pharmacol.* **2017**, *805*, 25–35.
- (a) Abbassi, R.; Johns, T. G.; Kassiou, M.; Munoz, L. *Pharmacol. Ther.* **2015**, *151*, 87–98. (b) Ma, Y.; Wink, M. *Phytother. Res.* **2010**, *24*, 146–9.
- Vishwakarma, V.; New, J.; Kumar, D.; Snyder, V.; Arnold, L.; Nissen, E.; Hu, Q.; Cheng, N.; Miller, D.; Thomas, A. R.; Shnyder,

- Y.; Kakarala, K.; Tsue, T. T.; Girod, D. A.; Thomas, S. M. *Sci. Rep.* **2018**, *8*, 12163.
- (20) Atteya, R.; Ashour, M. E.; Ibrahim, E. E.; Farag, M. A.; El-Khamisy, S. F. *Mech. Ageing Dev.* **2017**, *161*, 141–148.
- (21) Ramsay, R. R.; Popovic-Nikolic, M. R.; Nikolic, K.; Uliassi, E.; Bolognesi, M. L. *Clin. Transl. Med.* **2018**, *7*, 3.
- (22) Petrelli, A.; Giordano, S. *Curr. Med. Chem.* **2008**, *15*, 422–432.
- (23) Bose, P.; Dai, Y.; Grant, S. *Pharmacol. Ther.* **2014**, *143*, 323–36.
- (24) Qin, H. T.; Li, H. Q.; Liu, F. *Expert Opin. Ther. Pat.* **2017**, *27*, 621–636.
- (25) Kim, H. Y. S.; Lee, S. M. *Eur. J. Pharm. Sci.* **2012**, *45*, 708–715.
- (26) Serafim, T. L.; Carvalho, F. S.; Marques, M. P.; Calheiros, R.; Silva, T.; Garrido, J.; Milhazes, N.; Borges, F.; Roleira, F.; Silva, E. T.; Holy, J.; Oliveira, P. J. *Chem. Res. Toxicol.* **2011**, *24*, 763–774.
- (27) Whent, M.; Huang, H.; Xie, Z.; Lutterodt, H.; Yu, L.; Fuerst, E. P.; Morris, C. F.; Yu, L. L.; Luthria, D. J. *J. Agric. Food Chem.* **2012**, *60*, 2129–2135.
- (28) Serafim, T. L.; Marques, M. P.; Borges, F.; Oliveira, P. J. *J. Theor. Exp. Pharm.* **2008**, *1*, 3–13.
- (29) Cione, E.; Tucci, P.; Senatore, V.; Perri, M.; Trombino, S.; Iemma, F.; Picci, N.; Genchi, G. *J. Bioenerg. Biomembr.* **2008**, *40*, 19–26.
- (30) Lane, A. A.; Chabner, B. A. *J. Clin. Oncol.* **2009**, *27*, 5459–5468.
- (31) (a) Gryder, B. E. *Future Med. Chem.* **2012**, *4*, 1369–1370.
(b) Marks, P. A. *Expert Opin. Invest. Drugs* **2010**, *19*, 1049–66.
- (32) Huang, M.; Liu, G. *Cancer Lett.* **1998**, *135*, 97–105.
- (33) Shu, Y. J.; Bao, R. F.; Wu, X. S.; Weng, H.; Ding, Q.; Cao, Y.; Li, M. L.; Mu, J. S.; Wu, W. G.; Ding, Q. C.; Liu, T. Y.; Jiang, L.; Hu, Y. P.; Tan, Z. J.; Wang, P.; Liu, Y. B. *Anti-Cancer Agents Med. Chem.* **2014**, *14*, 1136–1145.
- (34) Sha, M.; Ye, J.; Zhang, L. X.; Luan, Z. Y.; Chen, Y. B.; Huang, J. *X. Pharmacology* **2014**, *93*, 39–46.
- (35) Lu, J.; Qin, Q.; Zhan, L.; Liu, J.; Zhu, H.; Yang, X.; Zhang, C.; Xu, L.; Liu, Z.; Wang, D.; Cui, H.; Meng, C.; Cai, J.; Cheng, H.; Sun, X. *J. Pharmacol. Sci.* **2014**, *126*, 56–65.
- (36) Choudhary, G. S.; Al-Harbi, S.; Almasan, A. *Methods Mol. Biol.* **2015**, *1219*, 1–9.
- (37) Yu, Z.; Jie, H.; Li, Z. *Med. Chem. Res.* **2013**, *22*, 2505–2510.
- (38) Sun, S. Y. *Autophagy* **2010**, *6*, 184–5.
- (39) Lu, Y.; Zhang, R.; Liu, S.; Zhao, Y.; Gao, J.; Zhu, L. *Eur. J. Pharmacol.* **2016**, *15*, 130–8.
- (40) Wang, F.; Ma, H.; Liu, Z.; Huang, W.; Xu, X.; Zhang, X. *Biomed. Pharmacother.* **2017**, *92*, 672–680.
- (41) Rodon, J.; Dienstmann, R.; Serra, V.; Tabernero, J. *Nat. Rev. Clin. Oncol.* **2013**, *10*, 143–153.
- (42) Ling, Y.; Xu, C.; Luo, L.; Cao, J.; Feng, J.; Xue, Y.; Zhu, Q.; Ju, C.; Li, F.; Zhang, Y.; Zhang, Y.; Ling, X. *J. Med. Chem.* **2015**, *58*, 9214–9227.